Materials Research. 2025; 28(suppl. 1):e20250129
DOI: https://doi.org/10.1590/1980-5373-MR-2025-0129

Isothermal Fatigue Characterization of P91 Steel Under Load Control

Yvens S. Sebastiany[a], *Antonio R. Faria Neto*[a]*, *Marcelo S. Martins* [a], *José Elias Tomazini*[a], *Mark Barkey*[b]

[a]*Universidade Estadual Paulista, Faculdade de Engenharia e Ciências, Guaratinguetá, SP, Brasil.*
[b]*The University of Alabama, College of Engineering, Tuscaloosa, EUA.*

Received: January 10, 2025; Revised: April 05, 2025; Accepted: April 11, 2025

P91 steels are widely used in power plants. They were developed in a context of increasing process temperatures to increase efficiency and reduce CO_2 emissions into the atmosphere. In this sense, the energy industry aims to increase its efficiency and process control, for which temperature control is essential and welding thermocouples in P91 steel pipes may be necessary. In this context, this study aims to evaluate, in a preliminary way, the influence of welding thermocouples in P91 steel specimens subjected to fatigue testing. The results showed that in general there is a decrease in fatigue life, more prominent for 90 and 80% of the load. In addition, the insertion of defects such as welding points increases the probability of the initiation of fatigue cracks in the welded areas due to loss of properties. From 70% of the load onwards, infinite fatigue life was achieved for the welded and as suplied cases, and in both conditions the same fracture shape was obtained, observed macroscopically.

Keywords: *P91 steel, Fatigue cracks, Thermocouples, Macroscopic analysis, Welding influence.*

1. Introduction

The 1970s were a milestone in the development of materials and technologies, especially with regard to steel, which was driven by the automotive and energy industries and led these advances. These initiatives occurred due to the need to reduce the industry's dependence on oil. First, we can highlight the oil crisis of 1973, when the Organization of the Petroleum Exporting Countries (OPEC) stopped exporting to the United States (US). This crisis was due to the US leaving the gold standard – which caused losses to OPEC, and to the Americans' support for Israel against Egypt and Syria in the Yom Kippur War[1]. Furthermore, there was great concern about CO_2 emissions into the atmosphere. In this sense, the automobile industry needed a lighter and more efficient vehicle, reducing oil consumption and consequently the emission of polluting gases. To this end, they worked on the development of advanced materials[1-4].

In the same sense, power plants have invested in advanced materials to increase efficiency and reduce CO_2 emissions into the atmosphere[5,6]. Increasing the efficiency of these industries depends on increasing operating temperature and pressure. However, the main problem associated with increasing operating temperature, pressure is related to the suitability of the material, since the application of materials at this temperature, and pressure level can cause microstructural transformations that lead to failure of the materials in service[7-9].

To achieve these objectives of reducing CO_2 emissions with increased efficiency in the energy industries, at the end of the 1970s, P91 steel was developed. P91 steel is a high strength steel that is being widely used in conventional and nuclear power plants, ideal for high temperatures. Regarding its microstructure, the P91 steel is a martensitic alloy steel that contains 9% chromium and 1% molybdenum, hence the name P91[10]. It has high ductility and can withstand temperatures up to 600°C. It also has a better resistance to oxidation than its predecessor, the P22 steel, and may have a longer fatigue life in use. It is an excellent material for pressurized parts and piping, such as steam stations and boilers[11].

Many studies address the welding process in P91 steels. These materials, when welded and applied at high temperatures, can present failures, compromising the projects. Khajuria et al.[12] studied, based on simulations, the properties in subzones of Heat Affected Zones (HAZ). In this study, it can be observed that the HAZ is divided into Fine-Grained Heat Affected Zone (FGHAZ), Intercritical Heat Affected Zone (ICHAZ) and that the addition of boron improved the creep resistance due to the greater fraction of small grain boundaries and martensite. Khajuria et al.[12], also studied the effects of boron on P91 steel from mechanisms related to creep performance and observed that the addition of the element is beneficial for the material. Nguyen et al.[13] observed a significant reduction in fatigue life in welded P91 steels. This reduction was attributed to cracks generated at the interface of the base metal and the (ICHAZ).

In this sense, the main objective of this paper is to determine the fatigue life behavior of P91 steel under different conditions for a load-controlled test. The temperature is measured using welded K-type thermocouples (TCs) on the surface of the specimen. The influence of the welded thermocouples on the fatigue life of the specimens was also sought to be determined.

*e-mail: antonio.fariant@gmail.com

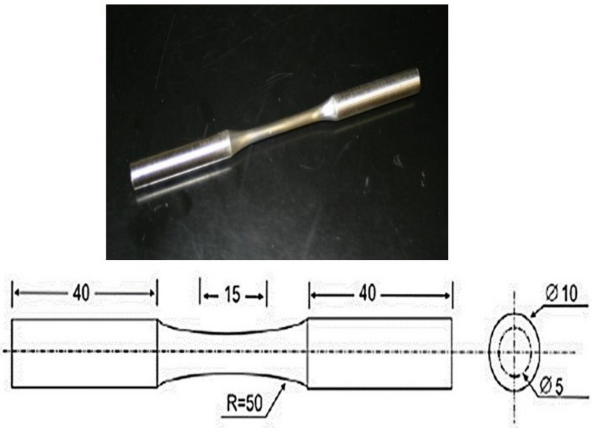

Figure 1. P91 specimen.

2. Materials and Methods

In this study, P91 specimens are fatigue tested in different circumstances. First, they were put in the testing machine in room temperature, without any TCs. Then they were tested the P91 specimens in room temperature using welded TCs in the surface.

2.1. Specimens

The P91 specimens used in this study were machined with a grip diameter of 10 mm and a diameter of 5 mm in the gauge section. The gripping sections are equally spaced. The Figure 1 shows one of the specimens.

2.2. Thermocouples

The thermocouples used in this study were the Lead Wire Type K 24 Ga., with insulation of fiberglass and being able to stand temperatures up to 900°F (482°C). Type K TCs are shown in Figure 2.

They are ribbon type TCs and have to be welded with the wires perpendicular to the specimen's axial direction, and parallel with respect to each other, with an ideal distance separation of 1 mm between each wire, as shown in the Figure 3.

2.3. Welding the thermocouples

In order to weld the TCs to the specimen's surface, it was used a TC Welder, with its value adjusted to 15 A to make a good weld. The Figure 4 shows the equipment.

2.4. Testing

The testing machine used in this study is shown in the Figure 5. It allows performing fatigue tests under load control and has an actuation force capacity up to 100kN. The Figure 5 shows the testing machine.

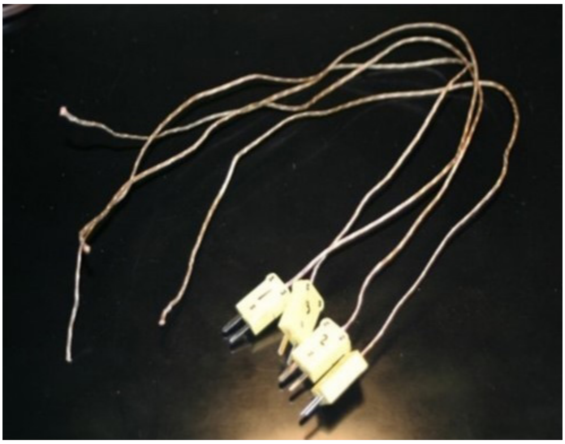

Figure 2. Type K ribbon TCs.

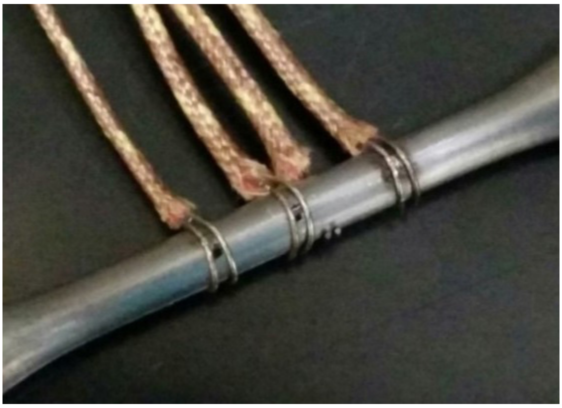

Figure 3. Welded TCs.

3. Results

The P91 specimens were tested under different load levels, as presented on Table 1.

For each different condition, two specimens were tested, and the fatigue life results are presented on Table 2.

From the results exposed on Table 2, it is possible to verify that the specimens with welded thermocouples (on the left) presented a shorter fatigue life in comparison to the other tested specimens for room temperature. One explanation is the fact that the specimens are heated during the welding process, what can change the materials microstructure, with different properties. The Figure 6 shows the plot Stress vs. Cycles to Failure for the specimens. With 70% of the load, infinite life was already reached, both for the specimens with welded thermocouple and for those without welded thermocouple. For the loads with 90% and 80%, the specimens presented approximately 138 and 280% more cycles on average to failure, respectively. This may indicate an influence of welding on the P91 material, some points are raised below.

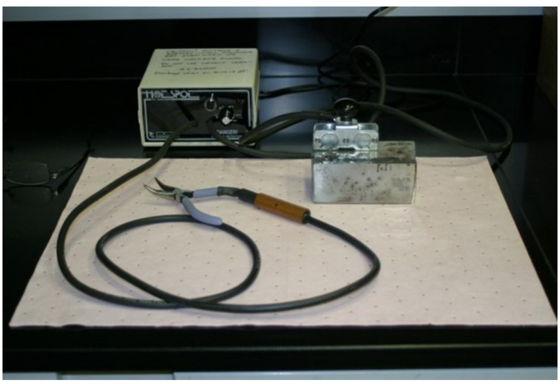

Figure 4. TC welder.

Nguyen et al.[13] in their studies on fatigue and crack distribution mechanism observed that in welded specimens

Figure 5. Testing machine.

Table 1. Different load levels applied on the specimens.

Stress (MPa)		F (N)	σmax (MPa)	σmin (R=0.1)	σm (Mpa)	σa (Mpa)
σrt	660.2	13,387.57	660.52	66.05	363.28	297.23
90%	594.47	12,048.81	594.47	59.45	326.96	267.51
80%	528.41	10,710.06	528.41	52.84	290.63	237.79
70%	462.36	09,371.30	462.36	46.24	254.30	208.06
60%	396.31	08,032.54	396.31	39.63	217.97	178.34
50%	330.26	06,693.79	330.26	33.03	181.64	148.62
40%	264.21	05,355.03	264.21	26.42	145.31	118.89
30%	198.16	04,016.27	198.16	19.82	108.99	089.17
20%	132.10	02,677.51	132.10	13.21	072.66	059.45
10%	066.05	01,338.76	066.05	06.61	036.33	029.72

Table 2. Fatigue life (N_f) of the tested specimens.

Room temperature							
P91 with TCs				P91 without TCs			
Specimen	Load	F (KN)	Cycles	Specimen	Load	F (N)	Cycles
P91-025-01	90%	12.05	83103	P91-025-11	90%	12.05	121,755
P91-025-02	90%	12.05	68727	P91-025-12	90%	12.05	88,476
P91-025-03	80%	10.71	82303	P91-025-13	80%	10.71	314,301
P91-025-04	80%	10.71	90411	P91-025-14	80%	10.71	159,997
P91-025-05	70%	9.371	1000000	P91-025-15	70%	9.371	1,000,000
P91-025-06	70%	9.371	1000000	P91-025-16	70%	9.371	1,000,000
P91-025-07	60%	8.033	1000000	P91-025-17	60%	8.033	1,000,000
P91-025-08	60%	8.033	1000000	P91-025-18	60%	8.033	1,000,000
P91-025-09	50%	6.694	1000000	P91-025-19	50%	6.694	1,000,000
P91-025-10	50%	6.694	1000000	P91-025-20	50%	6.694	1,000,000

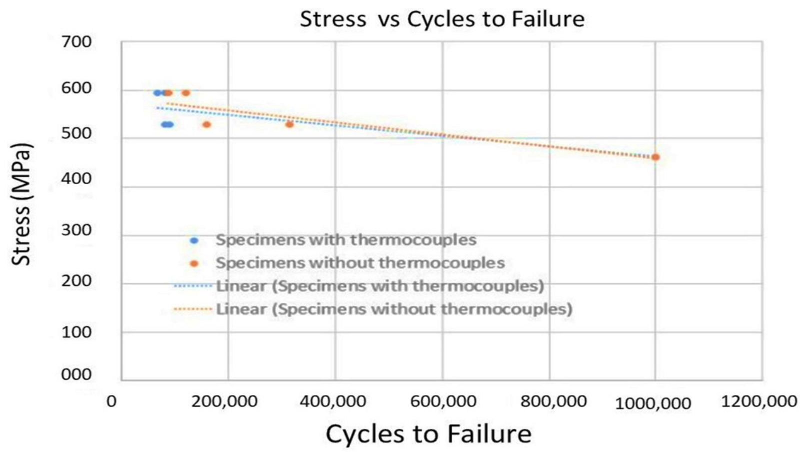

Figure 6. Plot stress vs Cycles to failure.

there is a significant reduction in fatigue life. Based on the peak temperatures experienced in the base material, phase transformations occur locally, inducing microstructure variations in the heat-affected zone (HAZ). However, sub-HAZs, such as fine-grained HAZ (FGHAZ) and ICHAZ, are often more critical points due to their low hardness and high susceptibility to premature failure under high temperature conditions[13,14]. Venugopal et al.[15] clarify in their paper that the welding process introduces very complex metallurgical and mechanical heterogeneities in this region due to solid-state phase transformations, residual stresses and heat treatments. In addition, the intercritical zone, a subzone of the HAZ, can accommodate coarse $M_{23}C_6$ carbides[15-17]. Das and Singh draw attention to the hydrogen embrittlement that can occur during welding of P91 steel. In their article, the authors reported that the presence of hydrogen promoted a reduction in elongation, fatigue life, greater absorption of plastic deformation energy and a higher softening rate for P91 steels[18].

To complement the fatigue study of P91 steel specimens welded with thermocouples, macroscopic analyses of the fractured region in the fatigue test were performed. This analysis can be used to indicate where the crack that fractured the specimen began.

3.1. Macroscopic analysis of the fractured region

To perform a preliminary assessment of the origin of the cracks in the fractured specimens, macroscopic images were taken on both sides of the fractured specimens in the fatigue test.

The Figure 7 shows the specimen P91-025-01 and P91-025-02, tested under a load of 90% (12.05 kN) and presented 83103 and 68727 cycles, respectively, before failure.

From the results obtained with the fatigue test and the macrograph obtained from the fractured specimens, the results are in line with the results obtained by Egner and Piotrowski[19] and Wu et al.[20] that P91 steel is subject to cyclic softening. Egner and Piotrowski also identified that the deformation in the sample depends on the temperature and at room temperature the predominance is tensile deformation. Therefore, as observed in Figure 7, the P91 steel presented ductile fracture for the P91 steel welded to the thermocouple, with 90% load. It is observed that the specimens broke outside the welding point. The Figure 8 shows the specimen P91-025-03 and P91-025-04, which was tested with a load of 80%, before failure.

Nguyen et al.[13] studied the fatigue behavior of welded P91 steels at elevated temperatures and observed that this behavior is similar to that of unwelded P91 steels tested at room temperature. In the tests, we observed that in addition to the shorter fatigue life, there is a change in the position of the fatigue crack, which in welded P91 steels occurs preferably at the ICHAZ interface, a subregion of the HAZ. The local reduction in microhardness, due to welding, can induce the localization of deformation due to the restricted deformation imposed by the surrounding hard materials, increasing the probability of crack initiation in this area[13,20-22].

It can be observed that, on average, the specimens tested with 90% of the load have a shorter life than those with 80% of the load, on average 10,000 cycles. However, what is observed is that with 80% the specimens broke from the welding point, agreeing with the authors who concluded that there is a greater probability of cracks in the HAZ. However, this does not rule out the existence of cracks in the base metal.

The Figure 9 shows the specimen P91-025-05 and P91-025-06, tested under a load of 70% (9.371 kN).

The specimens tested with 70% load or less showed an infinite fatigue life. However, cracks were observed from the welded point, in agreement with what was observed for specimens 03 and 04, with 80% load. Therefore, at room temperature, the consequences of welding are not as prominent as the application at high temperatures, but imply microstructural changes that result in a shorter fatigue life.

Figures 10 and 11 show the P91 steels without welded thermocouples with 90% and 80% load, respectively. In the images, it can be seen that the fractured region is similar to the regions shown in the welded P91 steels. Therefore, in the case of welded thermocouples, the weld point introduces defects

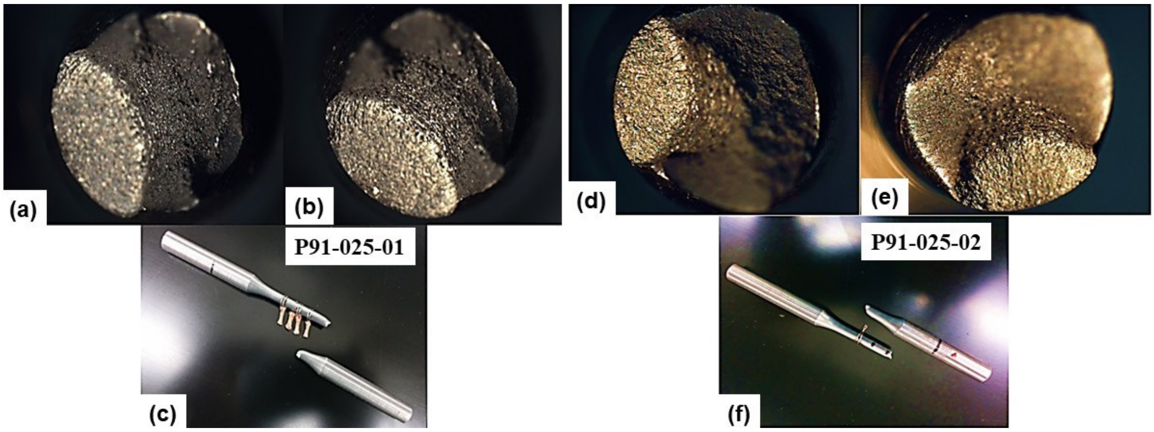

Figure 7. Broken specimen pictures. a) P91-025-01 fractured section taken by microscope; b) other half of the P91-025-01 fractured section; c) point of fracture; d) P91-025-02 fractured section taken by microscope; e) other half of the P91-025-02 fractured section; f) point of fracture.

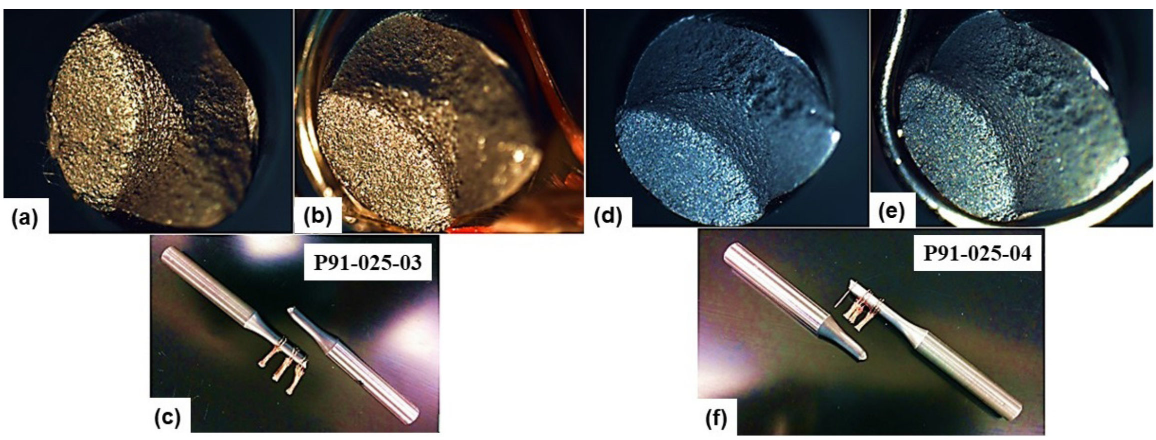

Figure 8. Broken specimen pictures. a) P91-025-03 fractured section taken by microscope; b) other half of the P91-025-03 fractured section; c) point of fracture; d) P91-025-04 fractured section taken by microscope; e) other half of the P91-025-04 fractured section; f) point of fracture.

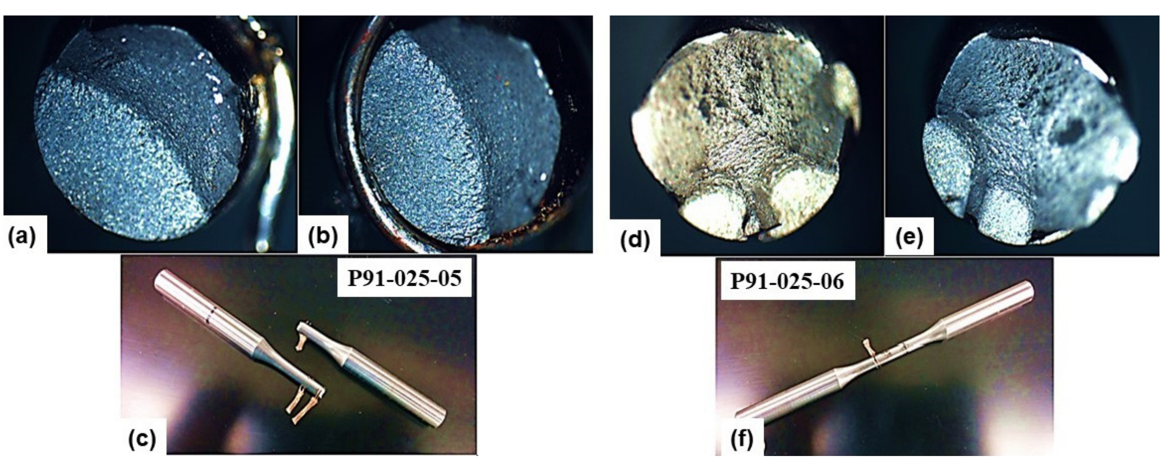

Figure 9. Broken specimen pictures. a) P91-025-05 fractured section taken by microscope; b) other half of the P91-025-05 fractured section; c) point of fracture; d) P91-025-06 fractured section taken by microscope; e) other half of the P91-025-05 fractured section; f) point of fracture.

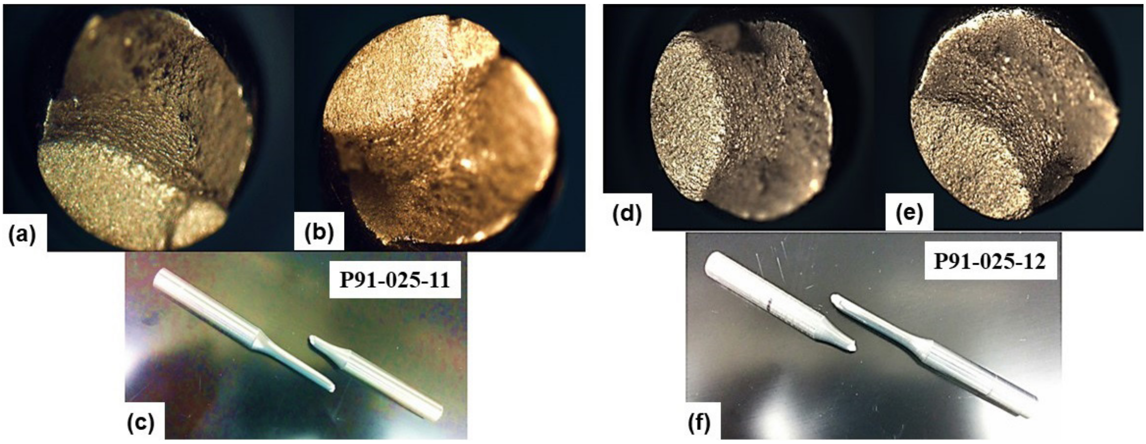

Figure 10. Broken specimen pictures. a) P91-025-11 fractured section taken by microscope; b) other half of the P91-025-11 fractured section; c) point of fracture; d) P91-025-12 fractured section taken by microscope; e) other half of the P91-025-12 fractured section; f) point of fracture.

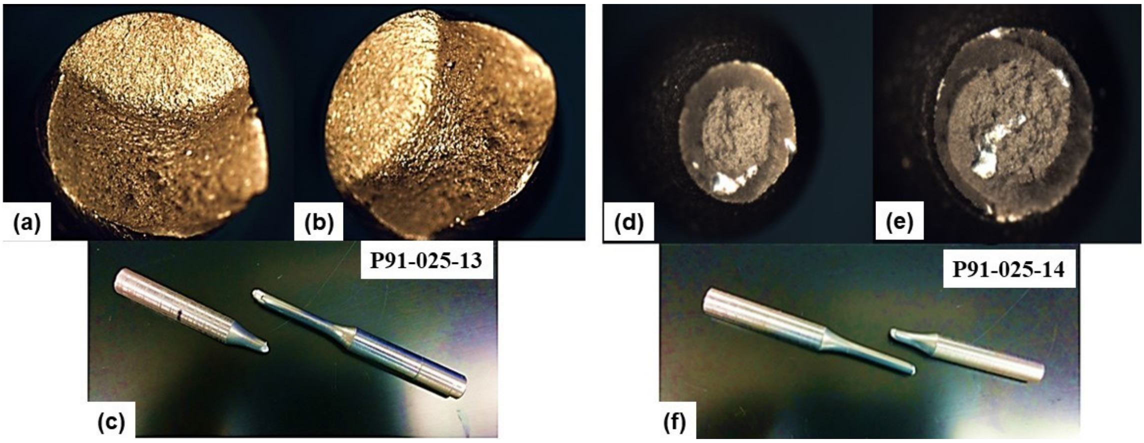

Figure 11. Broken specimen pictures. a) P91-025-13 fractured section taken by microscope; b) other half of the P91-025-13 fractured section; c) point of fracture; d) P91-025-14 fractured section taken by microscope; e) other half of the P91-025-14 fractured section; f) point of fracture.

that increase the probability of specimen rupture and reduce fatigue life, by introducing defects into the microstructure of the specimen. However, the dimension of the weld is not capable of altering the fracture mechanism and, as occurs for high-temperature applications, the presence of weld alters the crack initiation site.

Oliveira et al.[23] report that internal defects in materials, such as voids and microinclusions, act as stress concentrators and, consequently, are suitable locations for the nucleation of fatigue cracks. However, what can be observed, in advance in the macroscopic evaluation, is the initiation of cracks on the surface of the specimens, especially those containing welded thermocouples.

4. Conclusion

From the results obtained in this work, it can be concluded that, like most steels, P91 steels are susceptible to a decrease in response to mechanical stresses when welded.

Thermocouple welding for process monitoring reduces the fatigue life of P91 steel.

Thermocouple welding does not change the fracture type of P91 steel, despite reducing the fatigue life of the material.

For more in-depth evaluations of the fracture mechanism, other techniques should be performed, opening space for future work.

5. References

1. Faria AR No, Freitas FHC, Furtado AE, Fukugauchi CS, Pereira MS, Abdalla AJ. Desenvolvimento de aços avançados de alta resistência na indústria automobilística: importante alternativa para uma maior eficiência energética. In: Andrade PL, Ribeiro IM, editors. Ciência e engenharia de materiais: conceitos, fundamentos e aplicação. Guarujá: Científica Digital; 2021. p. 194-215.
2. Faria AR No, Dias EX, Fukugauchi CS, Martins MS, Pereira MS. Mechanical and microstructural characterization of class 800 complex phase steel before and after the laser welding process. J Manuf Mater Process. 2024;8(5):232.

3. Dias EX, Faria AR No, Castro TS, Martins MS, Pereira MS. Laser welding applied to complex phase steel. Warrendale: SAE Technical Paper; 2024.
4. Fukugauchi CS, Faria AR No, Ribeiro RB, Pereira MS. Microstructural characterization of dual and multiphase steels applied to automotive industry. In: 20th Brazilian Conference on Materials Science and Engineering; 2012 Nov 4-8; Joinville. Proceedings. Wollerau: Trans Tech Publications; 2014. p. 146-50.
5. Akhtar M, Khajuria A, Kumar VS, Gupta RK, Albert S. Evolution of microstructure during welding simulation of boron modified P91 steel. Phys Met Metallogr. 2019;120(7):672-85. http://doi.org/10.1134/S0031918X19070056.
6. Khajuria A, Bedi R, Kumar R. Investigation of impression creep deformation behavior of boron-modified P91 steel by high-end characterization techniques. In: Vishal SS, Uday SD, Noe A-B, editors. Manufacturing engineering: select proceedings of CPIE 2018. Singapore: Springer; 2019. p. 137-50.
7. Pandey C, Giri A, Mahapatra MM. Evolution of phases in P91 steel in various heat treatment conditions and their effect on microstructure stability and mechanical properties. Mater Sci Eng A. 2016;664:58-4. http://doi.org/10.1016/j.msea.2016.03.132.
8. Hald J. Microstructure and long-term creep properties of 9-12% Cr steels. Int J Press Vessels Piping. 2008;85(1-2):30-7. http://doi.org/10.1016/j.ijpvp.2007.06.010.
9. Yoshizawa M, Igarashi M. Long-term creep deformation characteristics of advanced ferritic steels for USC power plants. Int J Press Vessels Piping. 2007;84(1-2):37-43. http://doi.org/10.1016/j.ijpvp.2006.09.005.
10. Ennis PJ, Czyrska-Filemonowicz A. Recent advances in creep-resistant steels for power plant applications. Sadhana. 2003;28(3-4):709-30. http://doi.org/10.1007/BF02706455.
11. Saad AA, Sun W, Hyde TH, Tanner DWJ. Cyclic softening behaviour of a P91 steel under low cycle fatigue at high temperature. Procedia Eng. 2011;10:1103-8. http://doi.org/10.1016/j.proeng.2011.04.182.
12. Khajuria A, Akhtar M, Bedi R, Kumar R, Ghosh M, Das CR, et al. Influence of boron on microstructure and mechanical properties of Gleeble simulated heat-affected zone in P91 steel. Int J Press Vessels Piping. 2020;188:104246. http://doi.org/10.1016/j.ijpvp.2020.104246.
13. Nguyen TT, Yoon KB, Vu TT, Park J, Baek UB. On the changes in the low-cycle-fatigue life and cracking mechanism of P91 cross-weld specimens at elevated temperatures. Int J Fatigue. 2022;159:106833. http://doi.org/10.1016/j.ijfatigue.2022.106833.
14. Akhtar M, Khajuria A. Effects of prior austenite grain size on impression creep and microstructure in simulated heat affected zones of boron modified P91 steels. Mater Chem Phys. 2020;249:122847. http://doi.org/10.1016/j.matchemphys.2020.122847.
15. Venugopal S, Sasikala G, Kumar Y. Creep crack growth behavior of a P91 steel weld. Procedia Eng. 2014;86:662-8. http://doi.org/10.1016/j.proeng.2014.11.067.
16. Khajuria A, Akhtar M, Bedi R. Boron addition to AISI A213/P91 steel: preliminary investigation on microstructural evolution and microhardness at simulated heat-affected zone. Materialwiss Werkstofftech. 2022;53(10):1167-83. http://doi.org/10.1002/mawe.202100152.
17. Akhtar M, Khajuria A. The synergistic effects among crystal orientations, creep parameters, local strain, macro–microdeformation, and polycrystals' hardness of boron alloyed P91 steels. Steel Res Int. 2022;93(9):2100819. http://doi.org/10.1002/srin.202100819.
18. Das B, Singh A. Influence of hydrogen on the low cycle fatigue performance of P91 steel. Int J Hydrogen Energy. 2020;45(11):7151-68. http://doi.org/10.1016/j.ijhydene.2019.12.154.
19. Mroziński S, Egner H, Piotrowski M. Effects of fatigue testing on low-cycle properties of P91 steel. Int J Fatigue. 2019;120:65-72. http://doi.org/10.1016/j.ijfatigue.2018.11.001.
20. Wu D-L, Zhao P, Wang Q-Q, Xuan F-Z. Cyclic behavior of 9-12% Cr steel under different control modes in low cycle regime: a comparative study. Int J Fatigue. 2015;70:114-22. http://doi.org/10.1016/j.ijfatigue.2014.08.006.
21. Kumar R, Bedi R, Kumar M, Khajuria A. FEM-based computational studies on impression creep behavior of boron-added P91 steel. In: Mukhopadhyay AK, Mishra D, editors. Deformation and fracture in materials. Boca Raton: CRC Press; 2024. p. 218-42. http://doi.org/10.1201/9781003359364-14.
22. Akhtar M, Khajuria A. Probing true creep-hardening interaction in weld simulated heat affected zone of P91 steels. J Manuf Process. 2019;46:345-56. http://doi.org/10.1016/j.jmapro.2019.08.029.
23. Oliveira LG, Fukugauchi CS, Faria AR No, Guimarães VA. Avaliação e comparação microestrutural e das propriedades mecânicas entre um aço carbono e um aço microligado para aplicação em rodas ferroviárias. Materia (Rio J). 2020;25(2):e12647. http://doi.org/10.1590/s1517-707620200002.1047.